

# Environmental Research Letters



## LETTER

# Contrasting and interacting changes in simulated spring and summer carbon cycle extremes in European ecosystems

### OPEN ACCESS

#### RECEIVED

31 January 2017

#### REVISED

10 May 2017

#### ACCEPTED FOR PUBLICATION

17 May 2017

#### PUBLISHED

7 July 2017

Original content from this work may be used under the terms of the [Creative Commons Attribution 3.0 licence](#).

Any further distribution of this work must maintain attribution to the author(s) and the title of the work, journal citation and DOI.



Sebastian Sippel<sup>1,6</sup>, Matthias Forkel<sup>2</sup>, Anja Rammig<sup>3</sup>, Kirsten Thonicke<sup>4</sup>, Milan Flach<sup>1</sup>, Martin Heimann<sup>1</sup>, Friederike E L Otto<sup>5</sup>, Markus Reichstein<sup>1</sup> and Miguel D Mahecha<sup>1</sup>

<sup>1</sup> Max Planck Institute for Biogeochemistry, Hans-Knöll-Str. 10, 07745 Jena, Germany

<sup>2</sup> Department of Geodesy and Geoinformation, Technische Universität Wien, Gusshausstr. 2729, 1040 Vienna, Austria

<sup>3</sup> TUM School of Life Sciences Weihenstephan, Technische Universität München, Freising 85354, Germany

<sup>4</sup> Potsdam Institute for Climate Impact Research, Telegrafenberg, 14473 Potsdam, Germany

<sup>5</sup> Environmental Change Institute, University of Oxford, South Parks Road, Oxford OX1 3QY, United Kingdom

<sup>6</sup> Author to whom any correspondence should be addressed.

E-mail: [ssippel@bgc-jena.mpg.de](mailto:ssippel@bgc-jena.mpg.de)

**Keywords:** climate extremes, carbon cycle extremes, vegetation modelling, biogeosciences, climate change, ensemble modelling

Supplementary material for this article is available [online](#)

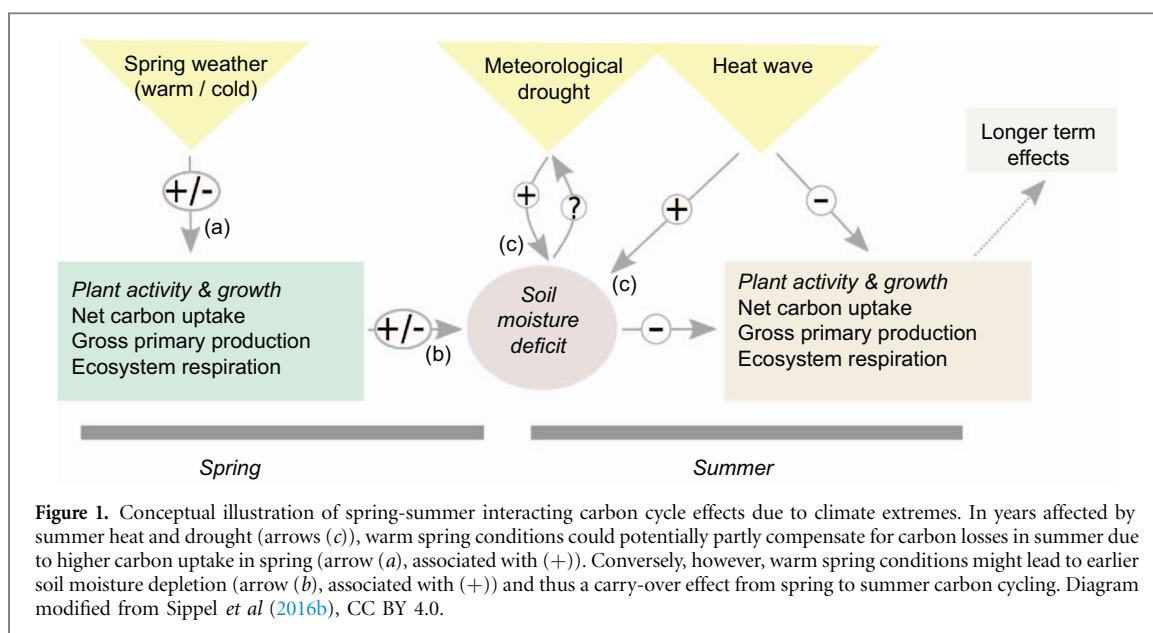
## Abstract

Climate extremes have the potential to cause extreme responses of terrestrial ecosystem functioning. However, it is neither straightforward to quantify and predict extreme ecosystem responses, nor to attribute these responses to specific climate drivers. Here, we construct a factorial experiment based on a large ensemble of process-oriented ecosystem model simulations driven by a regional climate model (12 500 model years in 1985–2010) in six European regions. Our aims are to (1) attribute changes in the intensity and frequency of simulated ecosystem productivity extremes (EPEs) to recent changes in climate extremes, CO<sub>2</sub> concentration, and land use, and to (2) assess the effect of timing and seasonal interaction on the intensity of EPEs. Evaluating the ensemble simulations reveals that (1) recent trends in EPEs are seasonally contrasting: spring EPEs show consistent trends towards increased carbon uptake, while trends in summer EPEs are predominantly negative in net ecosystem productivity (i.e. higher net carbon release under drought and heat in summer) and close-to-neutral in gross productivity. While changes in climate and its extremes (mainly warming) and changes in CO<sub>2</sub> increase spring productivity, changes in climate extremes decrease summer productivity neutralizing positive effects of CO<sub>2</sub>. Furthermore, we find that (2) drought or heat wave induced carbon losses in summer (i.e. negative EPEs) can be partly compensated by a higher uptake in the preceding spring in temperate regions. Conversely, however, carry-over effects from spring to summer that arise from depleted soil moisture exacerbate the carbon losses caused by climate extremes in summer, and are thus undoing spring compensatory effects. While the spring-compensation effect is increasing over time, the carry-over effect shows no trend between 1985–2010. The ensemble ecosystem model simulations provide a process-based interpretation and generalization for spring-summer interacting carbon cycle effects caused by climate extremes (i.e. compensatory and carry-over effects). In summary, the ensemble ecosystem modelling approach presented in this paper offers a novel route to scrutinize ecosystem responses to changing climate extremes in a probabilistic framework, and to pinpoint the underlying eco-physiological mechanisms.

## 1. Introduction

Climate variability and extremes are key features influencing terrestrial ecosystem functioning (Smith 2011, Reyer *et al* 2013, Baldocchi *et al* 2016). Climatic

extremes directly propagate into the biosphere through various eco-physiological pathways, for instance affecting plant phenological events (Jentsch *et al* 2009, Ma *et al* 2015) or carbon cycling from regional to global scales (Knapp *et al* 2002, Reichstein



*et al* 2013, Zscheischler *et al* 2014a, Frank *et al* 2015). Major climatic extreme events such as the European heat wave and drought in 2003 (Ciais *et al* 2005, Reichstein *et al* 2007), or droughts in North America (Schwalm *et al* 2012, Wolf *et al* 2016), Australia (Ma *et al* 2016) and the Amazon (Phillips *et al* 2009, Lewis *et al* 2011) consistently cause net carbon losses. However, because the number of directly observed large-scale extreme climate events and associated impacts on ecosystem productivity are rare, and because field experiments are often limited in extent and thus difficult to upscale to larger regions (Beier *et al* 2012), crucial uncertainties remain in our understanding of processes that control these phenomena.

Climatic extreme events are changing in magnitude and frequency (Alexander *et al* 2006, IPCC 2012), and these occur in addition to more gradual climatic changes in, e.g. seasonal variation (Stine *et al* 2009, Cassou and Cattiaux 2016) and climate trends. These changes, in tandem with non-linear feedbacks or lagged effects (Frank *et al* 2015), might impart decisive consequences for regional and global-scale carbon balances of terrestrial ecosystems (Reichstein *et al* 2013).

For example, the extreme summer drought 2012 in the contiguous United States caused losses in carbon uptake in summer (Wolf *et al* 2016) which were offset by warming-induced increases in spring carbon uptake, leading to a spring-summer compensation of the regional carbon balance (figure 1). Furthermore, Wolf *et al* (2016) hypothesized that earlier spring plant activity could have induced negative carry-over effects to summer productivity via soil-moisture deficits (figure 1), as suggested in Richardson *et al* (2010). However, as the evidence for seasonal compensation of extremes in Wolf *et al* (2016) is based on a single event only it remains uncertain whether such interacting effects can be expected generally for climate extremes

in summer. Long time series allowing a comprehensive study of additional *independent* climatic extreme events in spring and/or summer would be required as such lagged effects in ecosystem productivity could have simply occurred by chance.

Climate extremes may cause immediate or delayed responses in ecosystems (Frank *et al* 2015), but not all climate extremes lead to an extreme ecosystem response (Smith 2011). Therefore, systematic quantification and attribution of contemporary trends in ecosystem productivity extremes, including potential interactions of events, is required. Respective analysis on observations is often hindered by small sample sizes. Alternatively, large ensembles of climate-ecosystem model simulations might complement a 'case study type' assessment of extremes in the observational record because they allow exploration of how climate variability and extreme events are related to extreme ecosystem responses (Ciais *et al* 2005, Schwalm *et al* 2012, Wolf *et al* 2016). For example, multi-thousand member ensembles of climate simulations were used to analyse and attribute extreme climate events, such as the Russian heat wave in 2010 (Otto *et al* 2012), or to investigate the role of climate extremes in causing, e.g. floods (Pall *et al* 2011, Schaller *et al* 2016) and heat-health related issues (Mitchell *et al* 2016). This approach is appropriate when analysing the impact of climatic extreme events on ecosystem functions.

This study investigates two main objectives: our first objective is to systematically assess changes in EPEs in spring and summer using climate-ecosystem model ensemble simulations, and to attribute seasonal changes in EPEs to changes in climate extremes, atmospheric CO<sub>2</sub> and land-use change. Second, we focus on interactions between negative summer EPEs and the preceding spring conditions, and reinvestigate the outlined spring compensation and carry-over effects in years affected by negative summer EPEs on

regional carbon cycling from a climate-ecosystem ensemble modeling perspective, and provide a model-based interpretation and generalization of these effects.

## 2. Data and methods

The methodological workflow of the study is as follows: we use a large ensemble of bias-corrected regional climate model simulations (section 2.1) to drive an ensemble of ecosystem model simulations (section 2.2) for six eco-physiologically different European regions. Factorial model simulations are set up (section 2.3) and used to disentangle climatic and non-climatic drivers of seasonal changes in EPEs, and to scrutinize respective spring-summer interacting carbon cycle effects (section 2.4).

### 2.1. Regional climate model simulations and physically consistent bias correction

The core ingredient to the present study is an ensemble of regional climate simulations over Europe that cover 26 years of transient climate change (1985–2010) and 800 ensemble members in each year (i.e. 20 000 members in total) based on perturbed initial conditions. Climate model simulations have been generated through distributed computing on citizen scientists' computers ([www.climateprediction.net/weatherathome](http://www.climateprediction.net/weatherathome)), using the global general circulation model HadAM3P ( $1.875^\circ \times 1.25^\circ 15$  min resolution, 19 vertical levels) and a dynamically downscaled regional model version (HadRM3P,  $0.44^\circ \times 0.44^\circ \times 5$  min resolution, Massey *et al* (2015)) in atmosphere-only mode. Hence, the model is driven by observed sea surface temperatures, sea ice fractions, the solar cycle, and the observed atmospheric composition (greenhouse gases, aerosols, ozone, see Massey *et al* (2015) for further details). The present experimental setup has been used to assess and attribute changes in climatic extreme events and its impacts in various sectors (Otto *et al* 2012, Sippel and Otto 2014, Schaller *et al* 2016, Mitchell *et al* 2016), because the large available sample size allows scrutiny of even small changes in the odds of climatic extreme events. The European summer climate in HadRM3P and other climate models is frequently too hot and dry (Massey *et al* 2015). To alleviate this issue, we apply a resampling-based bias correction that preserves the physical consistency in the ensemble simulations (for details see Sippel *et al* (2016a)): A Gaussian kernel fitted over 1985–2010 mean summer area-averaged temperatures in the ERA-Interim dataset (Dee *et al* 2011) in each of the six European regions (online supplementary table S1) is used as a constraint for resampling 500 ensemble members in each year. The resampling procedure improves the representation of summer climate in HadRM3P substantially, but reduces the available sample size of the ensemble

and cannot account for all possible biases (Sippel *et al* 2016a).

### 2.2. Terrestrial ecosystem simulations: model description

The process-based Lund–Potsdam–Jena managed Land dynamic model (LPJmL, Version 3.5) simulates terrestrial vegetation dynamics (growth, competition and mortality), land–atmosphere fluxes of carbon (gross and net primary productivity, ecosystem respiration) and water (evaporation, transpiration, interception) in natural ecosystems (Sitch *et al* 2003) and under human land use (Bondeau *et al* 2007). Carbon allocation in LPJmL follows the fully coupled photosynthesis and water balance scheme of the BIOME3 model (Haxeltine and Prentice 1996), i.e. the photosynthetic light-use efficiency is subject to environmental controls via co-limiting light-limited enzyme regeneration and rubisco-limited enzyme-kinetic rates (Haxeltine and Prentice 1996). Respiration from plant compartments follows a modified Arrhenius relationship (Lloyd and Taylor 1994). Heterotrophic decomposition of litter and soil carbon pools depends additionally on soil moisture and follows first-order kinetics (Sitch *et al* 2003). LPJmL consists of 11 natural plant functional types and 13 crop functional types that differ in their bioclimatic limits and ecophysiological parameters. Here, we run LPJmL with an improved hydrology scheme (Gerten *et al* 2004, Schaphoff *et al* 2013), human land use (Bondeau *et al* 2007), agricultural water use (Rost *et al* 2008), and an improved phenology module (Forkel *et al* 2014). Phenology and photosynthesis-related parameters have been optimized against remote sensing observations resulting in an improved simulation of natural vegetation greenness dynamics (Forkel *et al* 2015). LPJmL ensemble simulations are performed at a monthly temporal and at  $0.5^\circ$  spatial resolution. The spinup procedure consists of 1200 years by randomly concatenating individual ensemble members (sampled from the first ten available years, 1986–1995) with transient  $\text{CO}_2$  concentration and land use.

#### 2.2.1. Region selection

All ensemble simulations are conducted for six individual regions in Europe that broadly sample the spectrum of variability of vegetation productivity in Europe (online supplementary figure S1, available at [stacks.iop.org/ERL/12/075006/mmedia](http://stacks.iop.org/ERL/12/075006/mmedia)), revealed from seasonal cycles in the satellite observed Fraction of Photosynthetically Active Radiation (FPAR) taken from the MODIS FPAR product (Myneni *et al* 2002). Spring (March–May) and summer (July–September) cover very different seasonality patterns in FPAR (figure 2). The LPJmL ensemble reproduces seasonal dynamics of vegetation phenology at the regional scale and the regional gradient in FPAR dynamics (figure 2).

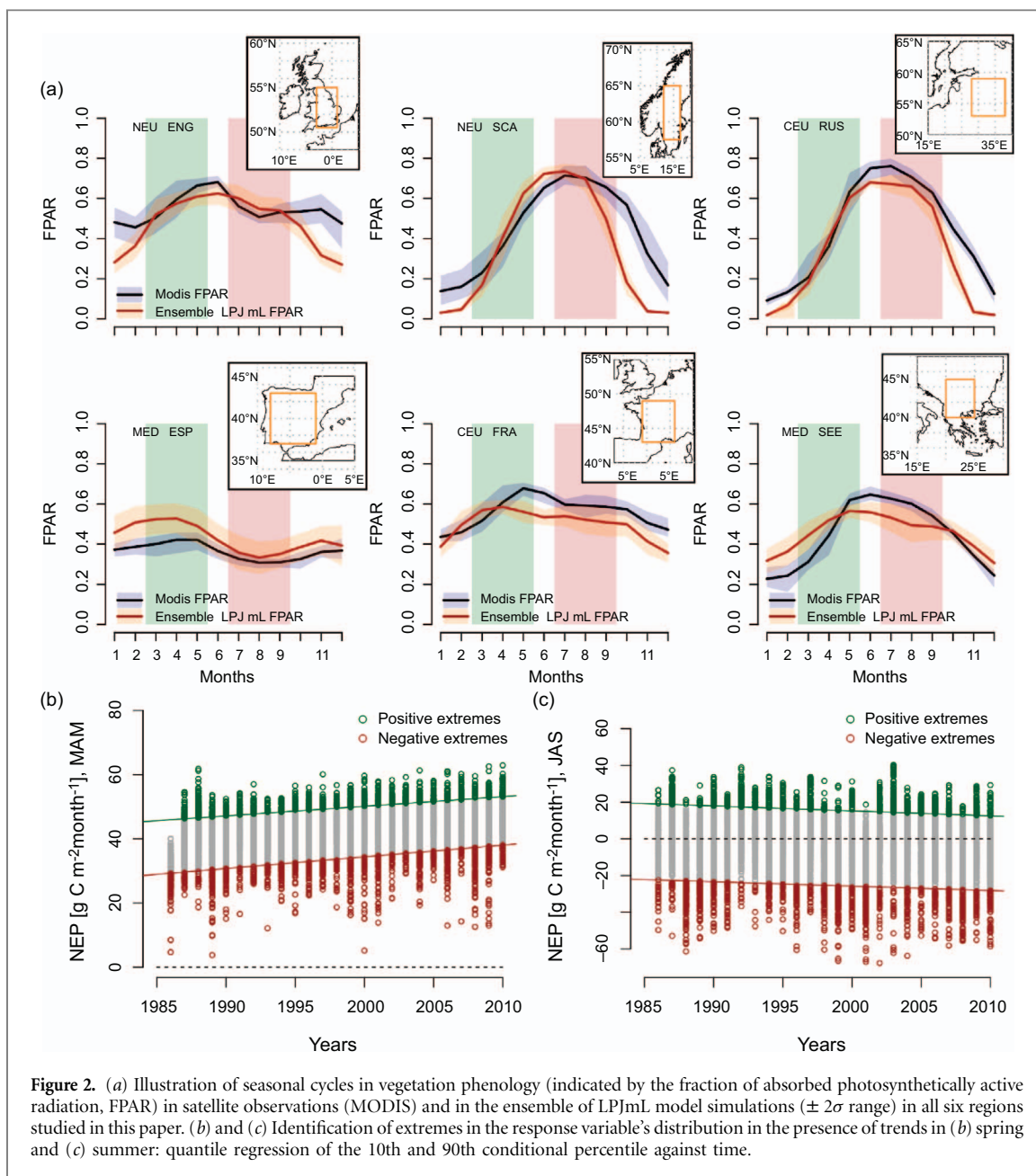


**Figure 2.** (a) Illustration of seasonal cycles in vegetation phenology (indicated by the fraction of absorbed photosynthetically active radiation, FPAR) in satellite observations (MODIS) and in the ensemble of LPJmL model simulations ( $\pm 2\sigma$  range) in all six regions studied in this paper. (b) and (c) Identification of extremes in the response variable's distribution in the presence of trends in (b) spring and (c) summer: quantile regression of the 10th and 90th conditional percentile against time.

**Table 1.** Overview over factorial model simulations<sup>a</sup>.

Scenario name	CO <sub>2</sub>	Land-use	Climate	Section
All	transient CO <sub>2</sub>	transient land-use	transient climate	3.1–3.3
CONSTCO <sub>2</sub>	constant CO <sub>2</sub> <sup>b</sup>	transient land-use	transient climate	3.1–3.2
CONSTLU	transient CO <sub>2</sub>	constant land-use <sup>c</sup>	transient climate	3.1–3.2
CONSTLUCO <sub>2</sub>	constant CO <sub>2</sub> <sup>b</sup>	constant land-use <sup>c</sup>	transient climate	3.1–3.2
SPRINGRAND	transient CO <sub>2</sub>	transient land-use	transient climate, spring randomization <sup>d</sup>	3.3

<sup>a</sup> Each factorial simulation is conducted for 1986–2010 climate and propagated through the entire climate ensemble.

<sup>b</sup> fixed to 345 ppm in 1985.

<sup>c</sup> fixed to 1985 land-use values.

<sup>d</sup> Ensemble members have been randomly concatenated on June 1st in each year ('random spring', but meteorological summer and autumn are identical to the other scenarios).

### 2.3. Factorial model simulations

The factorial set of climate–ecosystem model simulations (table 1) is based on a standard run ('All'), in which LPJmL is run with all drivers, including

transient CO<sub>2</sub> concentrations and human land-use (Fader *et al* 2010). Moreover, LPJmL is run separately for constant CO<sub>2</sub> ('CONSTCO<sub>2</sub>'), constant land-use ('CONSTLU'), and both constant CO<sub>2</sub> and land-use

(‘CONSTLUCO<sub>2</sub>’). In this factorial, ensemble-based setup the differences between these runs are used to disentangle and pinpoint climatic and non-climatic (CO<sub>2</sub>, land-use) drivers of contemporary changes in EPEs (sections 3.1 and 3.2). Lastly, to investigate carry-over effects from spring conditions to EPEs in summer (section 3.3), an additional LPJmL simulation driven by randomised spring climatic conditions (‘SPRING-RAND’) is conducted. This step consists of randomly concatenating members of the climate ensemble between summer and spring (on June 1st) within each year such that summer meteorology remains identical to the ‘All’ run, but spring conditions are different. Hence, the difference in summer carbon cycling between ‘All’ and ‘SPRINGRAND’ is driven by lagged effects from spring in the ecosystem model.

## 2.4. Analysis methodology

### 2.4.1. Selection of extreme events

All individual ensemble members are averaged to regional and seasonal means for further analysis. EPEs are sampled directly from the tail of the response variable distribution (Smith 2011), which is either gross primary productivity (GPP) or net ecosystem productivity (NEP) in the present study. Let  $x_{i,t,s,fac}$  denote the response variable  $x$  ( $x \in \{GPP, NEP\}$ ), an arbitrary ensemble member  $i$ , in year  $t$ , season  $s$ , and from any factorial run  $fac$  (region is not indexed separately to lighten the notation). Ensemble members in which the response variable exceeds or falls below a given threshold in the ‘All’ simulations are labelled as positive and negative EPEs ( $x_{j,t,s,fac}^{+extreme}$  and  $x_{j,t,s,fac}^{-extreme}$ , respectively). The index  $j$  runs only over ensemble members within in a given category ( $^{-extreme}$  or  $^{+extreme}$ ). In section 3.1, an illustrative extreme value analysis is conducted by fitting a generalized Pareto distribution (GPD) to extremes in the response variable, where the GPD constitutes a suitable limit distribution for such peak-over-threshold selection of extreme values (Coles *et al* 2001). These statistical fits are derived from the ‘All’ simulations separately for the response variables’s lower and upper tails (negative and positive EPEs) using a 5th and 95th quantile threshold to identify EPEs, and separately for each season and two decadal periods (1986–1995 and 2001–2010).

In sections 3.2 and 3.3, a quantile regression of the 10th (90th) conditional percentile against time in the ‘All’ simulation is performed (Cade and Noon, 2003) to identify EPEs relative to time-dependent thresholds, thus accounting for potential trends in the 25 year period. This yields a selection of 1250 EPEs (out of 12 500 members) for each response variable, region, and season (see figures 2(b) and (c) for an illustration).

### 2.4.2. Attribution to drivers of change

In section 3.1 (figure 3(b)–(e)), the effects of individual factors on changes in EPEs (CO<sub>2</sub>:  $\Delta x_{CO_2_s}^{-extreme}$ , land-use:  $\Delta x_{LU_s}^{-extreme}$ , climate:  $\Delta x_{climate_s}^{-extreme}$ ,

indicated here exemplarily only for negative extremes) between both periods and in season  $s$  are teased out by computing the difference between both time periods of the averaged individual effects from the factorial simulations (averages over any specific dimension (.) are denoted as  $\bar{x}$ ):

$$\Delta x_{CO_2_s}^{-extreme} = (\bar{x}_{\dots,2001-2010,s,All}^{-extreme} - \bar{x}_{\dots,2001-2010,s,CONSTCO_2}^{-extreme}) - (\bar{x}_{\dots,1986-1995,s,All}^{-extreme} - \bar{x}_{\dots,1986-1995,s,CONSTCO_2}^{-extreme}) \quad (1)$$

$$\Delta x_{LU_s}^{-extreme} = (\bar{x}_{\dots,2001-2010,s,All}^{-extreme} - \bar{x}_{\dots,2001-2010,s,CONSTLU}^{-extreme}) - (\bar{x}_{\dots,1986-1995,s,All}^{-extreme} - \bar{x}_{\dots,1986-1995,s,CONSTLU}^{-extreme}) \quad (2)$$

$$\Delta x_{climate_s}^{-extreme} (\bar{x}_{\dots,2001-2010,s,CONSTLUCO_2}^{-extreme} - \bar{x}_{\dots,1986-1995,s,CONSTLUCO_2}^{-extreme}) \quad (3)$$

In section 3.2, the contribution of changes in CO<sub>2</sub>, land-use and climate to trends in EPEs are estimated individually for each tail, response variable, region and season. We assume linear trend slopes over the 25 year period and computed these in both tails separately (illustrated here for the negative tail,  $\beta_{All_s}^{-extreme}$ ),

$$\beta_{All_s}^{-extreme} = \frac{\Delta(x_{\dots,s,All}^{-extreme})}{\Delta t} \quad (4)$$

The contribution of trends in CO<sub>2</sub> ( $\beta_{CO_2_s}^{-extreme}$ ), land-use ( $\beta_{LU_s}^{-extreme}$ ), and climate ( $\beta_{climate_s}^{-extreme}$ ) to changes in the response variable is determined from factorial model simulations, i.e.

$$\beta_{CO_2_s}^{-extreme} = \frac{\Delta(x_{\dots,s,All}^{-extreme} - x_{\dots,s,CONSTCO_2}^{-extreme})}{\Delta t} \quad (5)$$

$$\beta_{LU_s}^{-extreme} = \frac{\Delta(x_{\dots,s,All}^{-extreme} - x_{\dots,s,CONSTLU}^{-extreme})}{\Delta t} \quad (6)$$

$$\beta_{climate_s}^{-extreme} = \frac{\Delta(x_{\dots,s,CONSTLUCO_2}^{-extreme})}{\Delta t} \quad (7)$$

To further examine *climate-related* drivers of change in ecosystem productivity, we analyse the individual contribution of trends in temperature, precipitation and radiation to  $\beta_{climate_s}$ . A simple statistical attribution framework is presented in the online supplementary data based on the ‘CONSTLUCO<sub>2</sub>’ scenario (supplementary section S1.2).

### 2.4.3. Spring–summer interacting carbon cycle effects due to climate extremes

In section 3.3, we identify all ensemble members that experience a negative EPE in summer (June–September, i.e.  $x_{j,t,s,All}^{-extreme,JJAS}$ ) using a time-dependent 10th percentile threshold. To detect spring compensation effects, we analyse the preceding spring conditions in the identified ensemble members in terms of

ecosystem productivity anomalies that might potentially alleviate carbon losses in summer. Furthermore, the contribution of carry-over effects from spring to negative summer EPEs (e.g. via soil moisture depletion) is disentangled using factorial model simulations by analysing the difference between the 'All' and 'SPRINGRAND' simulations, i.e. with identical summer meteorology in both factorial simulations, but randomised spring meteorology. Hence, we compute spring–summer carry-over effects as the difference between the identified negative summer EPEs in both scenarios.

### 3. Results

In this section, we firstly illustrate in one region how large ensembles of climate–ecosystem model simulations can be used to study EPEs (section 3.1) and, secondly present a systematic assessment of spring and summer trends in EPEs and an attribution to drivers (section 3.2). Lastly, we investigate spring–summer interacting carbon cycle effects due to climate extremes (section 3.3).

#### 3.1. An illustrative attribution analysis of ecosystem productivity extremes

The probability distributions of monthly GPP and NEP from the LPJmL ensemble in CEU-FRA for an earlier (1986–1995) and a more recent (2001–2010) period reveal an overall upward shift of GPP and NEP in spring but more nuanced changes in summer (figure 3(a) for NEP and online supplementary figure S5(a) for GPP). To investigate these changes in more detail, we apply an extreme value analysis to the tails of the probability distributions in both periods. Return time plots (figures 3(b)–(e)) for NEP and figures S5 (b)–(e) for GPP have been used widely in event attribution studies (National Academies of Sciences, Engineering and Medicine, 2016) to scrutinize the tails of a distribution by plotting the magnitude of an extreme event as a function of return time. Here, an event in the upper (lower) tail with an average return time of 20 years corresponds to a 95th (5th) percentile event when using annual data.

Differences between the blue and orange lines in figures 3(b)–(e) indicate how the likelihood of EPEs occurring has changed between the two compared decades for a given season and extreme type. In spring, terrestrial ecosystems exhibit an increase in GPP and NEP under extreme conditions in the upper and lower tail of the distribution in the more recent period (both tails shifted upward for any given return time, figures 3 (b) and (d) and figures S5(b) and (d)). These increases are driven by a roughly equal positive contribution of climate and CO<sub>2</sub> changes in the upper tail, and a larger contribution of climate change in the lower tail, in particular for GPP (figure S5(d)). Changes in the tails of the GPP distribution between both periods that are

induced by individual drivers in the ecosystem model are largely additive, i.e. the average contribution of changes in CO<sub>2</sub>, land-use, and climate added to the statistical model for the 1986–1995 tail matches the statistical fit for the 2001–2010 tail (figures 3(b)–(e) and figure S5).

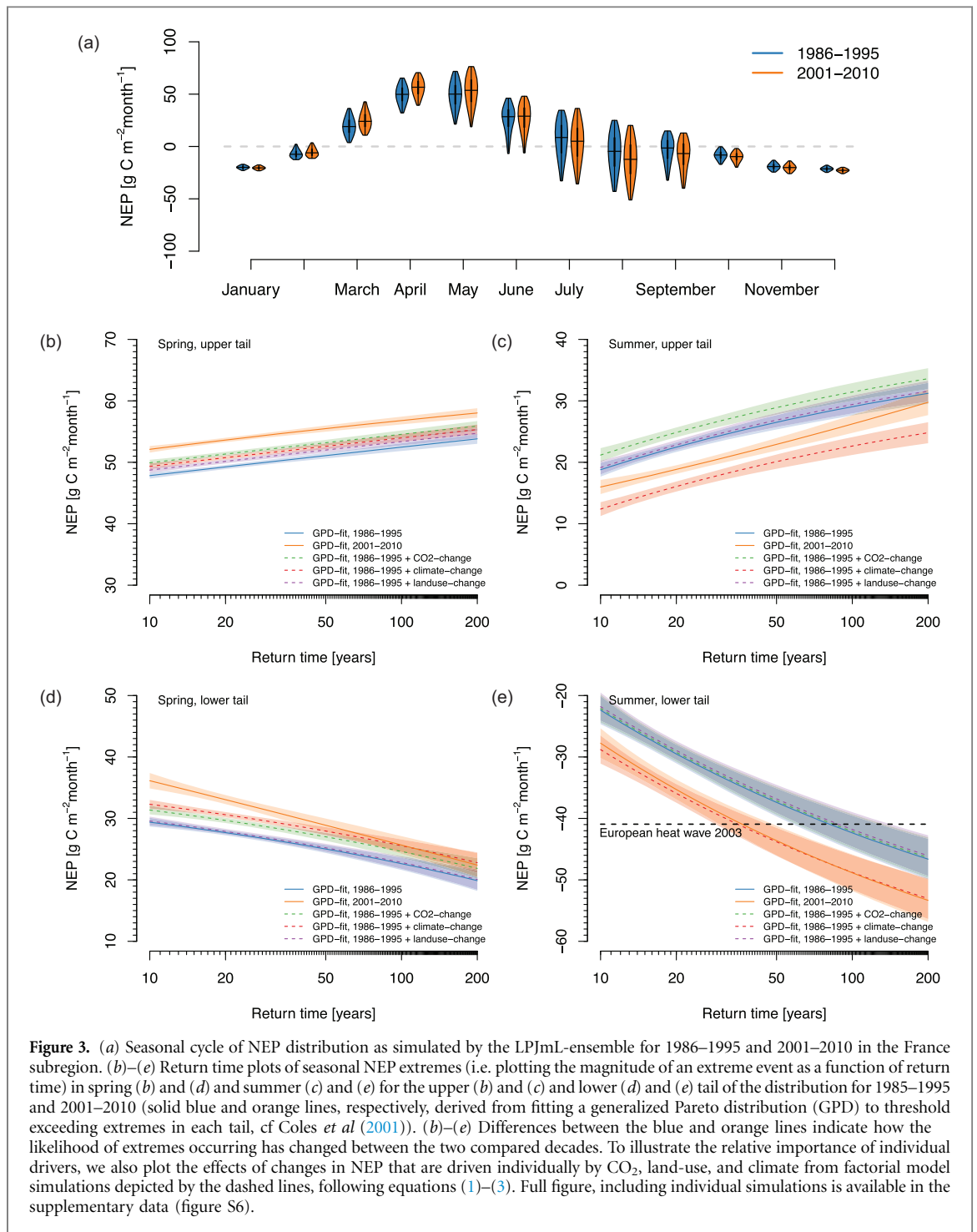
Changes in summer GPP are close to neutral, because the negative response to climate change is compensated by a positive contribution of CO<sub>2</sub>. NEP has significantly reduced (figures 3(c) and (e)), predominantly due to negative climate effects. For illustration, the European heat wave and drought of 2003 (figure 2(e), dashed horizontal line) results in a roughly 1-in-80 year event in the 1985–1995 decade but is already a 1-in-35 year event in the recent period. While the difference between the two decades used in this study is not comparable to a counterfactual climate simulation as utilised in other attribution studies (Mitchell *et al* 2016) it is reasonable to assume that the main difference in the climate simulations and thus NEP simulations comes from anthropogenic climate change.

Because ecosystem responses to climate extremes are often highly nonlinear and asymmetric depending on the type of extreme, changes in the likelihood of EPEs as discussed here are likely different from risk ratios based on meteorological variables alone (Stott *et al* 2004, Stott *et al* 2013). This study therefore exemplifies a simulation of the whole chain of events from meteorology to ecosystem responses in extreme event attribution (Stone and Allen 2005) and presents a framework for studying extreme ecosystem impacts.

#### 3.2. Attribution of trends in ecosystem productivity extremes

Across all six European regions, trends towards increased gross productivity in spring for both positive and negative EPEs from 1986–2010 confirm a general upward shift in the GPP distribution (figure 4(a)) that is driven by both climate and CO<sub>2</sub> changes. The pattern of an upward shift in spring is also found for NEP, but to a smaller extent that can be explained by a smaller sensitivity to recent changes in CO<sub>2</sub> and climate (figure 4(b)). This is because recent climate change and CO<sub>2</sub> fertilisation are not only enhancing primary productivity in spring but also ecosystem respiration, causing a smaller net response. Positive GPP trends are generally more than twice as large as NEP trends, i.e. less than half of the increased carbon uptake remains in the system after increased respiratory losses are accounted for, which is a consistent pattern for both positive and negative EPEs.

In summer, the response of ecosystem productivity to recent climate change reverses (with few exceptions), but remains positive for CO<sub>2</sub> changes: Hence, predominantly negative ecosystem productivity responses to recent climate change are balanced by a positive response to CO<sub>2</sub> change, causing a mix of slightly increased (two regions), close-to-neutral



(three regions) and reduced (one region) gross carbon uptake. Summer increases are confined to energy-limited regions in northern Europe (NEU-SCA and CEU-RUS) and more pronounced for the upper tail of GPP because the response of positive EPEs to recent climate change is marginally positive (in contrast to the other regions, figure 4(a)). Similar to spring, summer NEP trends are generally smaller in magnitude than GPP trends, and almost exclusively negative. The observed negative trends in summer ecosystem productivity and EPEs are most pronounced in water-limited regions in southern Europe (MED-SEE, MED-ESP, CEU-FRA) with

relatively similar trend slopes in the upper and lower tail. The energy-limited regions in northern Europe experience reduced summer productivity under negative EPEs, but small increases in NEP under positive EPEs due to slightly different climate responses in the upper and lower tail (figure 4(b)).

Overall, LPJmL ensemble simulations reveal that seasonally contrasting responses of EPEs to changing climate conditions will be a crucial factor in determining regional-scale carbon balances in the near future. Further analyzing climate-induced *trends* in spring and summer ecosystem productivity ( $\beta_{\text{climateMAM}}$  and  $\beta_{\text{climateJAS}}$ ) in the online supplementary data

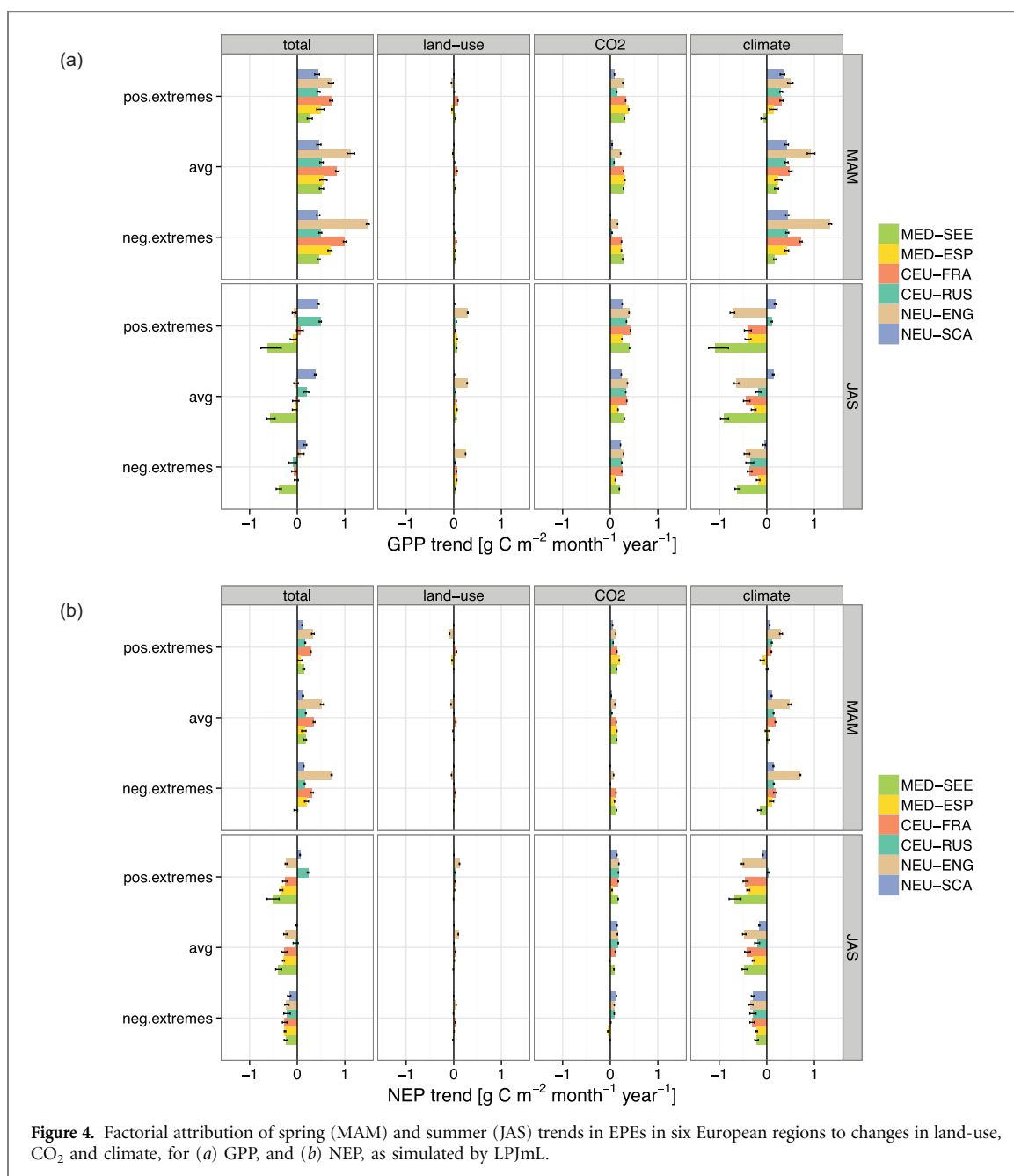


**Figure 4.** Factorial attribution of spring (MAM) and summer (JAS) trends in EPEs in six European regions to changes in land-use, CO<sub>2</sub> and climate, for (a) GPP, and (b) NEP, as simulated by LPJmL.

(sections S1.2 and S2.2) reveals that climate-induced positive productivity trends are mostly driven by warming temperatures in spring (GPP: figure S7, NEP: figure S8), whereas the ecosystem response to summer warming is negative for NEP and GPP across Europe (except GPP in NEU-SCA).

### 3.3. Elucidating spring–summer interacting carbon cycle effects due to climate extremes

In 2012, the contiguous United States experienced a very warm spring followed by an extreme summer drought. Wolf *et al* (2016) hypothesized that warmer spring conditions and elevated spring plant activity might have induced soil moisture deficits, thereby exacerbating the impacts of summer drought (figure 1). Here, we analyse lagged effects in all ensemble members that experience extreme reductions in

summer productivity<sup>7</sup> (negative EPEs). Specifically, we investigate

- whether productivity losses induced by summer droughts are (increasingly) compensated by warmer spring conditions (‘spring compensation’, conceptual link (a) in figure 1), and
- whether spring–summer ‘carry over effects’ via soil moisture depletion further exacerbate negative EPEs in summer (conceptual link (b) in figure 1)?

<sup>7</sup> The subregion over Spain is excluded from the analysis because seasonality in ecosystem productivity differs strongly from other European regions, see figure 2.

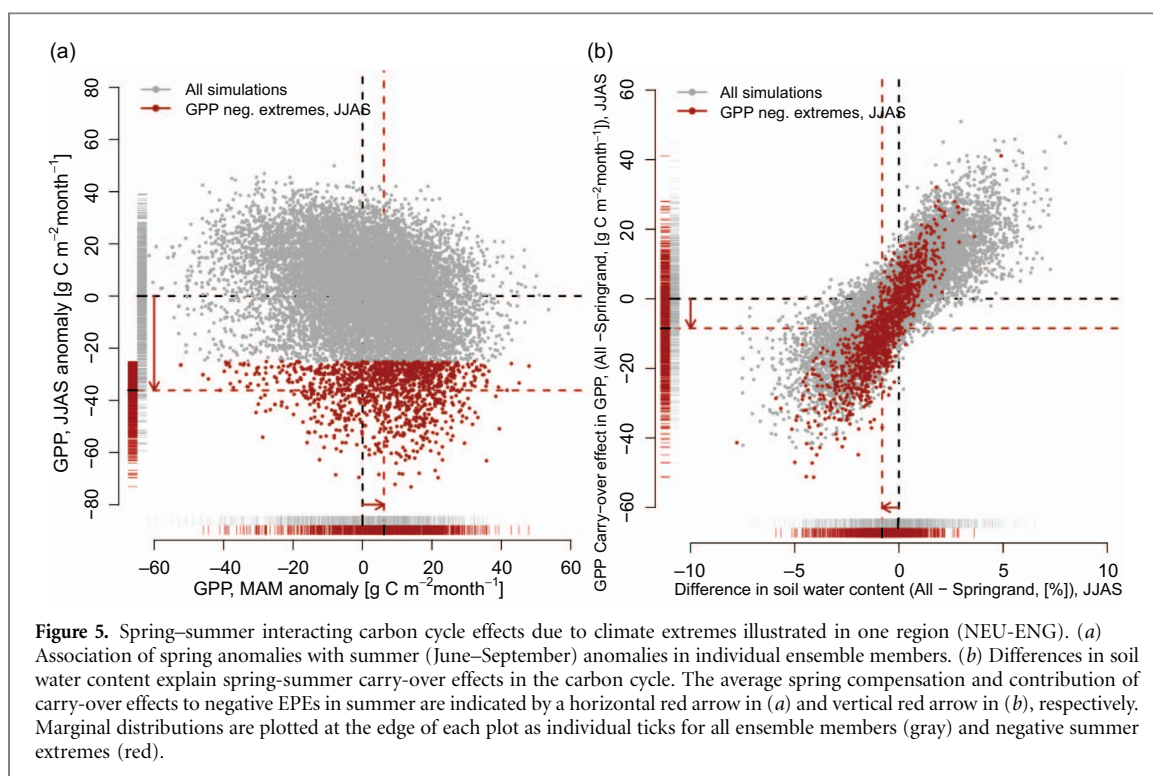


**Table 2.** Spring compensation of summer extremes in GPP and contribution of dynamical effects.

Region	Variable	Summer extreme Mean ( $\text{gC m}^{-2}$ $\text{month}^{-1}$ )	Spring compensation			Carry-over effect		
			Mean ( $\text{gC m}^{-2}$ $\text{month}^{-1}$ )	Mean <sup>a</sup> (% of summer anomaly)	Trend <sup>a,b</sup> (% $\text{year}^{-1}$ )	Mean ( $\text{gC m}^{-2}$ $\text{month}^{-1}$ )	Mean (% of summer anomaly)	Trend <sup>b</sup> (% $\text{year}^{-1}$ )
NEU-SCA	GPP	−24.0	5.6	19.0	1.7*	−2.8	11.5	−0.1
NEU-ENG	GPP	−36.1	6.2	13.2	2.1*	−8.5	23.5	−0.4*
CEU-RUS	GPP	−38.2	5.7	11.3	1.0*	−3.3	8.3	0.0
CEU-FRA	GPP	−33.7	1.0	2.7	1.7*	−4.8	14.4	−0.1
MED-SEE	GPP	−34.3	−2.1	−4.6	0.7*	−3.1	8.6	0.1
NEU-SCA	NEP	−19.5	2.0	7.8	0.3*	−1.9	9.1	0.2*
NEU-ENG	NEP	−27.2	1.5	3.8	1.2*	−5.1	19.1	−0.8*
CEU-RUS	NEP	−32.2	1.4	3.3	0.5*	−2.0	6.0	0.0
CEU-FRA	NEP	−27.3	−1.6	−4.3	1.0*	−2.9	11.1	−0.4*
MED-SEE	NEP	−24.9	−3.5	−10.4	0.4*	−2.1	8.7	−0.4*

<sup>a</sup> The sign is reversed for the computation of spring compensation relative to the summer anomaly for ease of understanding.

<sup>b</sup> Significance of the trend slopes at the 5% confidence level is indicated by an asterisk (\*).

The conditional selection of summer extremes over NEU-ENG (figure 5(a)) shows that negative summer extremes can be preceded by various ecosystem productivity conditions in spring (figure 5(a)), i.e. there is no obvious deterministic link. However, there is indeed a *probabilistic* link between carbon cycling under summer extremes and the preceding spring productivity conditions, as four out of five European regions show, on average, increased spring GPP that compensates to a small extent for summer reductions (2.7%–19.0% average compensation, table 2), but smaller effects are observed for NEP (−4.3% to +7.8%). The MED-SEE region is an exception where summer extremes co-occur with on average reduced spring productivity (−4.6% in GPP

and −10.4% in NEP of the summer anomaly are in addition lost in spring). Moreover, elevated ecosystem productivity in spring (GPP, and less so NEP) is increasingly compensating reductions in summer productivity in all European regions over the past 25 years (figure 6), albeit average spring compensation of negative EPEs in summer can only account for a fraction of the summer anomaly. These trends might be a consequence of seasonally contrasting trend slopes (sections 3.1 and 3.2).

### 3.3.1. Is there a causal link between spring carbon cycling and summer extremes?

Carry-over effects from spring to summer contribute on average 8.3%–23.5% for GPP (6.0%–19.1% for

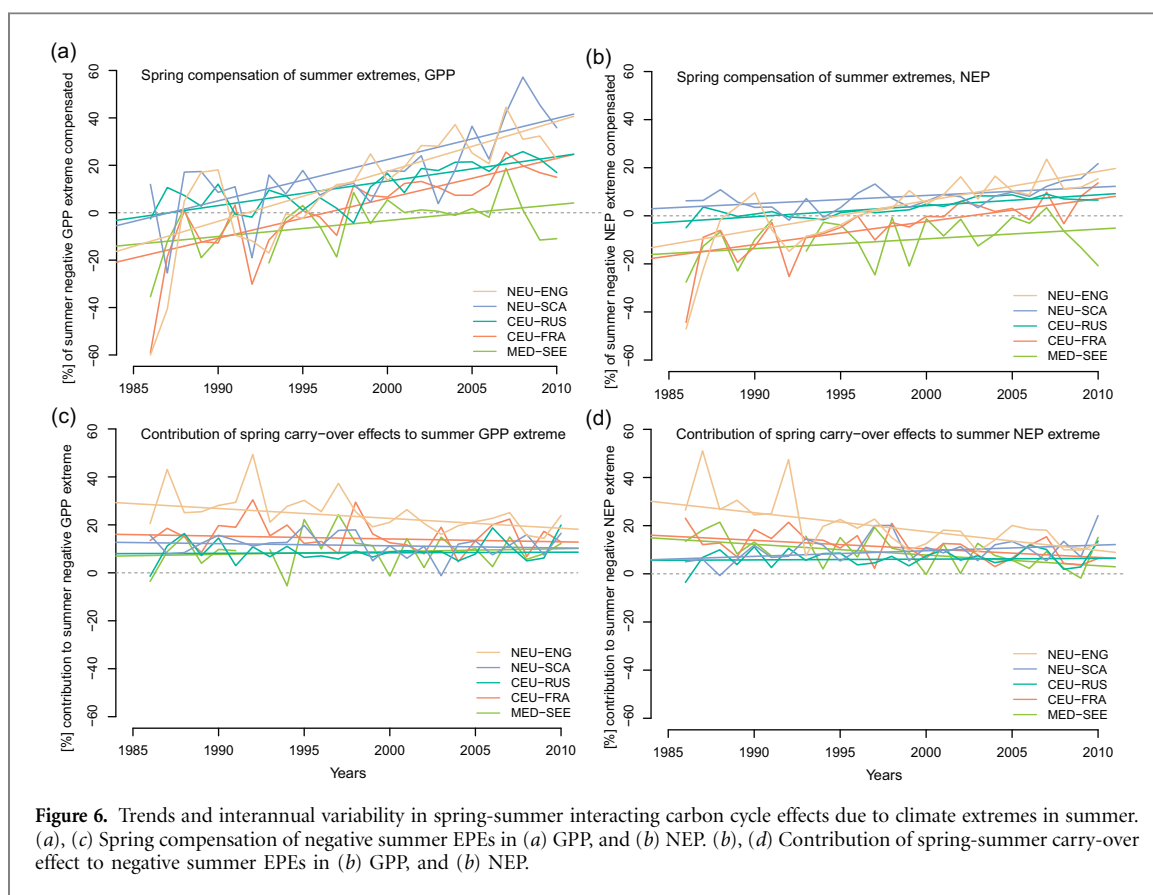


**Figure 6.** Trends and interannual variability in spring-summer interacting carbon cycle effects due to climate extremes in summer. (a), (c) Spring compensation of negative summer EPEs in (a) GPP, and (b) NEP. (b), (d) Contribution of spring-summer carry-over effect to negative summer EPEs in (b) GPP, and (b) NEP.

NEP) to the magnitude of extreme productivity reductions in summer (negative EPEs, see figure 5(b) for an illustration). This carry-over contribution is revealed by analysing differences in summer EPEs in the ‘All’ and ‘SPRINGRAND’ simulations (table 1), where summer meteorology is identical but spring conditions randomized in the latter simulation. Hence, summer ecosystem productivity extremes would be less severe if they would have been preceded by *random* spring conditions. The carry-over effects simulated by LPJmL are due to soil moisture depletion, because differences in soil moisture content explain a large fraction of the magnitude of carry-over effects across all regions (online supplementary table S2, figure 5(b) for NEU-ENG). These carry-over effects have been largely stable over the last 25 years (figure 6).

In summary, the analyses presented here provide an independent process model explanation and generalization of the observed seasonal compensation mechanism (Wolf *et al* 2016). However, we find that the average spring compensation of summer extremes is relatively small for GPP, almost neutral for NEP, and even negative (spring amplification of summer extreme) in MED-SEE for both GPP and NEP. Conversely, carry-over effects from spring to summer extremes via soil moisture play an important role in shaping simulated EPEs and exacerbate carbon cycle impacts on average. Hence, a substantial contribution of compensation effects (as observed for the 2012 US event, (Wolf *et al* 2016)) cannot generally be expected

at present in Europe, and the role of these effects remains to be quantified on larger spatial scales, including uncertain long term legacy effects of climate extremes (Anderegg *et al* 2015). Furthermore, positive compensation trends as found for recent years (figure 6) cannot continue indefinitely, simply because there are natural limits to shifts in ecosystem phenology (Körner and Basler, 2010) and plant physiological responses to warming (Norby and Luo 2004).

#### 4. Discussion

The results of our study provide evidence that EPEs in European ecosystems show a seasonally contrasting response to changes in climate when investigated using a large ensemble of ecosystem model simulations. Spring climatic changes tend to shift the GPP and NEP distribution upwards (including extremes in the upper and lower tails), whereas climatic changes in summer, most notably warming, lead to approximately neutral (GPP) or even negative trends (NEP), i.e. intensified carbon losses under climate extremes. Further, summer carbon losses as a result of climate extremes are partly compensated by a higher uptake in the preceding spring in temperate regions, but these spring compensatory effects are largely undone through a negative carry-over effect from spring to summer via depleted soil moisture, which further exacerbates summer carbon losses. Hence, our analyses provide a model generalization

and interpretation of seasonal compensation and carry-over effects of carbon-cycle extremes.

However, the results of the present analysis might be confined by the fact that the underlying climate ensemble is based on just one regional climate model and uncertainties related to simulated trends, changes in (individual) climate variables, potential feedback mechanisms, and the applied bias correction remain (Massey *et al* 2015, Sippel *et al* 2016a).

Ecosystem models are derived from well-established theory of plant-atmosphere carbon exchange (Bonan 2015), and are widely analysed in the context of climate extremes (Ciais *et al* 2005, Reichstein *et al* 2007, Zscheischler *et al* 2014a). Nonetheless, the results presented here can still be influenced by scale mismatches, where models scale carbon assimilation from leaf to the ecosystem scale (Rogers *et al* 2017), or ecophysiological processes are simulated without considering a diurnal cycle and averaged over 0.5° grid cell size.

Moreover, a possible caveat of the present study is that ecosystem and carbon cycle models tend to overestimate the response of terrestrial carbon cycling to drought conditions if compared to observations-based datasets (Huang *et al* 2016). LPJmL and related earlier versions have been shown to overestimate the sensitivity of ecosystem productivity to precipitation deficits in central European regions as compared to tree ring data (Babst *et al* 2013), albeit qualitative responses are largely captured (Rammig *et al* 2015). Temperature extremes that are not associated with precipitation deficits are not affected (Rammig *et al* 2015). On the continental scale in Europe, extremes in LPJmL simulated GPP respond more sensitively to climate extremes than data-driven products, but in a qualitatively consistent way considering for example the ratio between positive and negative GPP extremes in Europe (Zscheischler *et al* 2014b). In this context, comparing the upper and lower tail of simulated ecosystem productivity in this study (figure 3(c) vs. figure 3(e)) reveals that extreme carbon losses in the lower tail are larger in magnitude than gains due to positive EPEs for a given return period (slopes in the return time plots in the lower tail exceed those in the upper tail for both GPP and NEP). This asymmetry in EPEs is consistent with analyses at the continental and global scale in observations-based products (Zscheischler *et al* 2014b). Van Oijen *et al* (2014) compares ecosystem productivity simulations and the vulnerability to precipitation deficits to satellite observations of vegetation greenness and finds that LPJmL (and other vegetation models) largely reproduce spatial patterns across Europe. Furthermore, the LPJmL version used in the present study incorporates a phenology scheme that improves phenological dynamics and variability of FPAR (Forkel *et al* 2015), and thus might overcome one of the previously identified key weaknesses of earlier LPJmL versions (Mahecha *et al* 2010).

Nonetheless, the analysis and attribution of simulated EPEs ignores a number of ecosystem processes and potential feedbacks between these, as these are missing in the LPJmL ecosystem model (e.g. wind disturbance, pests, nitrogen and phosphorous limitations) and generally many ecosystem processes and feedbacks during climatic extreme events are still unknown or uncertain (Reichstein *et al* 2013, Frank *et al* 2015). Hence, model improvements can only be conducted in synthesis with improving our process understanding of climatic extreme events. Therefore, dedicated ecosystem manipulation experiments (Knapp *et al* 2002, Jentsch *et al* 2007, Beier *et al* 2012) will be crucial to evaluate and scrutinize model predictions.

Despite these caveats, we argue that the analyses and tools presented here are useful to investigate specific hypotheses related to extremes in terrestrial ecosystems. Our approach allows a physically consistent probabilistic assessment of extremes in ecosystem productivity. Because the outlined probabilities and return times of EPEs are based on one ecosystem model, they should not be taken at face value, but rather be regarded as an approach to scrutinize model sensitivities and attribute drivers behind contemporary changes in ecosystem risk on decadal time scales.

An application of the analysis metrics developed for this study to other process-oriented ecosystem models or data-driven approaches (Tramontana *et al* 2016) could be one way to sample respective ecosystem model uncertainties, and to further scrutinise various hypotheses about interacting and contrasting contemporary changes in the frequency and intensity of ecosystem productivity extremes. Thereby, our suggested ensemble analyses might complement state-of-the-art ecosystem risk assessments (Van Oijen *et al* 2014, Rolinski *et al* 2015) and possibly guide ecosystem manipulation experiments towards pinpointing the most relevant and uncertain drivers of contemporary change in ecosystem extremes.

## 5. Conclusion

In this paper, we illustrate large ensemble simulations of ecosystem productivity as a useful tool to explore variability and change in EPEs from a probabilistic perspective. The approach allows to identify the drivers of changes in EPEs using attribution-type analyses (Stott *et al* 2013) and to analyse interacting carbon cycle effects caused by climate extremes (i.e. compensatory and carry-over effects). We find contrasting trends in spring vs. summer carbon cycle extremes in six eco-physiologically different European regions. A recent upward shift in the distribution of spring ecosystem productivity (including extremes) can be attributed to recent climate warming and CO<sub>2</sub> increases, whereas in summer, ecosystem extremes are intensifying for NEP (i.e. more carbon lost to

the atmosphere under drought and heat conditions) and roughly stable for GPP, despite a positive response to increasing CO<sub>2</sub>. Despite these overarching trends, regional differences are emerging, in that water-limited regions in southern Europe show smaller trends in spring, hence benefitting to a smaller degree from warming, while negative trends in summer net ecosystem productivity and its extremes are least pronounced in temperature-limited northern regions.

Furthermore, spring GPP increasingly compensates negative EPEs in summer GPP in four out of five European regions. However, this compensation occurs only partly, on average in the range of 2.7%–19.0% of the summer anomaly, but depends on the definition of extremes (figure 5). Spring compensation effects and trends are smaller but mostly positive for NEP. Conversely, spring–summer carry-over effects exacerbate carbon cycle losses under summer extremes (contribution of 8%–23% in GPP and 6%–19% in NEP to summer anomaly), thereby counterbalancing and undoing positive compensation-related effects. Therefore, we expect that climate extremes increasing in frequency and intensity (IPCC 2012) might further exacerbate legacy effects of ecosystem extremes in the long term beyond the actual events (Anderegg *et al* 2015).

## Acknowledgments

We thank Nuno Carvalhais, Kazuhito Ichii, Martin Jung, Sonia I. Seneviratne, and Sebastian Wolf for helpful comments and discussions. We would like to thank our colleagues at the Oxford eResearch Centre for their technical expertise, the Met Office Hadley Centre PRECIS team for their technical and scientific support for the development and application of weather@home and all volunteers who have donated their computing time to climateprediction.net. ERA-Interim data provided courtesy ECMWF. This research has received funding from the European Commission Horizon 2020 BACI Project (Towards a Biosphere Atmosphere Change Index, grant No. 640176). SS is grateful to the German National Academic Foundation (Studienstiftung des Deutschen Volkes) for support and the International Max Planck Research School for Global Biogeochemical Cycles (IMPRS-gBGC) for training.

## References

- Alexander L *et al* 2006 Global observed changes in daily climate extremes of temperature and precipitation *J. Geophys. Res. Atmos.* **111** 1984–2012
- Anderegg W R *et al* 2015 Pervasive drought legacies in forest ecosystems and their implications for carbon cycle models *Science* **349** 528–32
- Babst F *et al* 2013 Site- and species-specific responses of forest growth to climate across the European continent *Global Ecol. Biogeogr.* **22** 706–17
- Baldocchi D, Ryu Y and Keenan T 2016 Terrestrial carbon cycle variability *F1000 Research* **5** 2371
- Beier C *et al* 2012 Precipitation manipulation experiments—challenges and recommendations for the future *Ecol. Lett.* **15** 899–911
- Bonan G 2015 *Ecological Climatology: Concepts and Applications* (New York: Cambridge University Press)
- Bondeau A *et al* 2007 Modelling the role of agriculture for the 20th century global terrestrial carbon balance *Glob. Change Biol.* **13** 679–706
- Cade B S and Noon B R 2003 A gentle introduction to quantile regression for ecologists *Front. Ecol. Environ.* **1** 412–20
- Cassou C and Cattiaux J 2016 Disruption of the European climate seasonal clock in a warming world *Nat. Clim. Change* **6** 589–94
- Ciais P *et al* 2005 Europe-wide reduction in primary productivity caused by the heat and drought in 2003 *Nature* **437** 529–33
- Coles S, Bawa J, Trenner L and Dorazio P 2001 *An Introduction to Statistical Modeling of Extreme Values* vol **208** (London: Springer)
- Dee D *et al* 2011 The ERA-Interim reanalysis: configuration and performance of the data assimilation system *Q. J. R. Meteorol. Soc.* **137** 553–97
- Fader M, Rost S, Müller C, Bondeau A and Gerten D 2010 Virtual water content of temperate cereals and maize: present and potential future patterns *J. Hydrol.* **384** 218–31
- Forkel M *et al* 2014 Identifying environmental controls on vegetation greenness phenology through model–data integration *Biogeosciences* **11** 7025–50
- Forkel M, Migliavacca M, Thonicke K, Reichstein M, Schaphoff S, Weber U and Carvalhais N 2015 Co-dominant water control on global inter-annual variability and trends in land surface phenology and greenness *Glob. Change Biol.* **21** 3414–35
- Frank D *et al* 2015 Effects of climate extremes on the terrestrial carbon cycle: concepts, processes and potential future impacts *Glob. Change Biol.* **21** 2861–80
- Gerten D, Schaphoff S, Haberlandt U, Lucht W and Sitch S 2004 Terrestrial vegetation and water balance-hydrological evaluation of a dynamic global vegetation model *J. Hydrol.* **286** 249–70
- Haxeltine A and Prentice I C 1996 BIOME3: an equilibrium terrestrial biosphere model based on ecophysiological constraints, resource availability, and competition among plant functional types *Glob. Biogeochem. Cycles* **10** 693–709
- Huang Y, Gerber S, Huang T and Lichstein J W 2016 Evaluating the drought response of CMIP5 models using global gross primary productivity, leaf area, precipitation, and soil moisture data *Glob. Biogeochem. Cycles* **30** 1827–46
- IPCC 2012 Summary for policymakers *Managing the Risks of Extreme Events and Disasters to Advance Climate Change Adaptation: Special Report of the Intergovernmental Panel on Climate Change* ed C Field *et al* (New York: Cambridge University Press)
- Jentsch A, Kreyling J and Beierkuhnlein C 2007 A new generation of climate-change experiments: events, not trends *Front. Ecol. Environ.* **5** 365–74
- Jentsch A, Kreyling J, Boettcher-Treschkow J and Beierkuhnlein C 2009 Beyond gradual warming: extreme weather events alter flower phenology of European grassland and heath species *Glob. Change Biol.* **15** 837–49
- Knapp A K, Fay P A, Blair J M, Collins S L, Smith M D, Carlisle J D, Harper C W, Danner B T, Lett M S and McCarron J K 2002 Rainfall variability, carbon cycling, and plant species diversity in a mesic grassland *Science* **298** 2202–5
- Körner C and Basler D 2010 Phenology under global warming *Science* **327** 1461–2
- Lewis S L, Brando P M, Phillips O L, van der Heijden G M and Nepstad D 2011 The 2010 Amazon drought *Science* **331** 554–4
- Lloyd J and Taylor J 1994 On the temperature dependence of soil respiration *Funct. Ecol.* **8** 315–23
- Ma X *et al* 2016 Drought rapidly diminishes the large net CO<sub>2</sub> uptake in 2011 over semi-arid Australia *Sci. Rep.* **6** 37747

- Ma X, Huete A, Moran S, Ponce-Campos G and Eamus D 2015 Abrupt shifts in phenology and vegetation productivity under climate extremes *J. Geophys. Res. Biogeosci.* **120** 2036–52
- Mahecha M D *et al* 2010 Comparing observations and process-based simulations of biosphere-atmosphere exchanges on multiple timescales *J. Geophys. Res. Biogeosci.* **115** G02003
- Massey N, Jones R, Otto F, Aina T, Wilson S, Murphy J, Hassell D, Yamazaki Y and Allen M 2015 weather@home-development and validation of a very large ensemble modelling system for probabilistic event attribution *Q. J. R. Meteorol. Soc.* **141** 1528–45
- Mitchell D, Heaviside C, Vardoulakis S, Huntingford C, Masato G, Guillod B P, Frumhoff P, Bowery A, Wallom D and Allen M 2016 Attributing human mortality during extreme heat waves to anthropogenic climate change *Environ. Res. Lett.* **11** 074006
- Myneni R *et al* 2002 Global products of vegetation leaf area and fraction absorbed par from year one of modis data *Remote Sens. Environ.* **83** 214–31
- National Academies of Sciences, Engineering and Medicine 2016 *Attribution of Extreme Weather Events in the Context of Climate Change* (Washington DC: National Academies Press)
- Norby R J and Luo Y 2004 Evaluating ecosystem responses to rising atmospheric CO<sub>2</sub> and global warming in a multi-factor world *New Phytol.* **162** 281–93
- Otto F, Massey N, Oldenborgh G, Jones R and Allen M 2012 Reconciling two approaches to attribution of the 2010 Russian heat wave *Geophys. Res. Lett.* **39** L04702
- Pall P, Aina T, Stone D A, Stott P A, Nozawa T, Hilberts A G, Lohmann D and Allen M R 2011 Anthropogenic greenhouse gas contribution to flood risk in England and Wales in autumn 2000 *Nature* **470** 382–5
- Phillips O L *et al* 2009 Drought sensitivity of the Amazon rainforest *Science* **323** 1344–7
- Rammig A, Wiedermann M, Donges J, Babst F, von Bloh W, Frank D, Thonicke K and Mahecha M 2015 Coincidences of climate extremes and anomalous vegetation responses: comparing tree ring patterns to simulated productivity *Biogeosciences* **12** 373–85
- Reichstein M *et al* 2013 Climate extremes and the carbon cycle *Nature* **500** 287–95
- Reichstein M *et al* 2007 Reduction of ecosystem productivity and respiration during the European summer 2003 climate anomaly: a joint flux tower, remote sensing and modelling analysis *Glob. Change Biol.* **13** 634–51
- Reyer C P *et al* 2013 A plant's perspective of extremes: terrestrial plant responses to changing climatic variability *Glob. Change Biol.* **19** 75–89
- Richardson A D *et al* 2010 Influence of spring and autumn phenological transitions on forest ecosystem productivity *Phil. Trans. R. Soc. Lond. B* **365** 3227–46
- Rogers A *et al* 2017 A roadmap for improving the representation of photosynthesis in earth system models *New Phytol.* **213** 22–42
- Rolinski S, Rammig A, Walz A, von Bloh W, Van Oijen M and Thonicke K 2015 A probabilistic risk assessment for the vulnerability of the European carbon cycle to weather extremes: the ecosystem perspective *Biogeosciences* **12** 1813–31
- Rost S, Gerten D, Bondeau A, Lucht W, Rohwer J and Schaphoff S 2008 Agricultural green and blue water consumption and its influence on the global water system *Water Resour. Res.* **44** 9
- Schaller N *et al* 2016 Human influence on climate in the 2014 southern England winter floods and their impacts *Nat. Clim. Change* **6** 627–34
- Schaphoff S, Heyder U, Ostberg S, Gerten D, Heinke J and Lucht W 2013 Contribution of permafrost soils to the global carbon budget *Environ. Res. Lett.* **8** 014026
- Schwalm C R *et al* 2012 Reduction in carbon uptake during turn of the century drought in western North America *Nat. Geosci.* **5** 551–6
- Sippel S and Otto F 2014 Beyond climatological extremes—assessing how the odds of hydrometeorological extreme events in south-east Europe change in a warming climate *Clim. Change* **125** 381–98
- Sippel S, Otto F, Forkel M, Allen M, Guillod B, Heimann M, Reichstein M, Seneviratne S, Thonicke K and Mahecha M D 2016a A novel bias correction methodology for climate impact simulations *Earth Sys. Dyn.* **7** 71
- Sippel S, Zscheischler J and Reichstein M 2016b Ecosystem impacts of climate extremes crucially depend on the timing *Proc. Natl Acad. Sci.* **113** 5768–70
- Sitch S *et al* 2003 Evaluation of ecosystem dynamics, plant geography and terrestrial carbon cycling in the LPJ dynamic global vegetation model *Glob. Change Biol.* **9** 161–85
- Smith M D 2011 An ecological perspective on extreme climatic events: a synthetic definition and framework to guide future research *J. Ecol.* **99** 656–63
- Stine A, Huybers P and Fung I 2009 Changes in the phase of the annual cycle of surface temperature *Nature* **457** 435–40
- Stone D A and Allen M R 2005 The end-to-end attribution problem: from emissions to impacts *Clim. Change* **71** 303–18
- Stott P A, Allen M, Christidis N, Dole R M, Hoerling M, Huntingford C, Pall P, Perlwitz J and Stone D 2013 Attribution of weather and climate-related events *Climate Science for Serving Society* (Dordrecht: Springer) pp 307–7
- Stott P A, Stone D A and Allen M R 2004 Human contribution to the European heatwave of 2003 *Nature* **432** 610–4
- Tramontana G *et al* 2016 Predicting carbon dioxide and energy fluxes across global fluxnet sites with regression algorithms *Biogeosciences* **13** 4291–313
- Van Oijen M *et al* 2014 Impact of droughts on the carbon cycle in European vegetation: a probabilistic risk analysis using six vegetation models *Biogeosciences* **11** 6357–75
- Wolf S *et al* 2016 Warm spring reduced carbon cycle impact of the 2012 US summer drought *Proc. Natl Acad. Sci.* **113** 5880–5
- Zscheischler J *et al* 2014a Impact of large-scale climate extremes on biospheric carbon fluxes: an intercomparison based on MSTMIP data *Global Biogeochem. Cycles* **28** 585–600
- Zscheischler J, Reichstein M, Harmeling S, Rammig A, Tomelleri E and Mahecha M D 2014b Extreme events in gross primary production: a characterization across continents *Biogeosciences* **11** 2909–24